Stability of C54 titanium germanosilicide on a silicon-germanium alloy substrate

Cite as: Journal of Applied Physics **77**, 5107 (1995); https://doi.org/10.1063/1.359321
Submitted: 11 November 1994 • Accepted: 01 February 1995 • Published Online: 17 August 1998

D. B. Aldrich, Y. L. Chen, D. E. Sayers, et al.

Stability of C54 titanium germanosilicide on a silicon-germanium alloy substrate

D. B. Aldrich, Y. L. Chen, D. E. Sayers, and R. J. Nemanich[a)]
Department of Physics, North Carolina State University, Raleigh, North Carolina 27695-8202

S. P. Ashburn and M. C. Öztürk
Department of Electrical and Computer Engineering, North Carolina State University, Raleigh, North Carolina 27695-7911

(Received 11 November 1994; accepted for publication 1 February 1995)

The stability of C54 $Ti(Si_{1-y}Ge_y)_2$ films in contact with $Si_{1-x}Ge_x$ substrates was investigated. The C54 $Ti(Si_{1-y}Ge_y)_2$ films were formed from the Ti-$Si_{1-x}Ge_x$ solid phase metallization reaction. It was determined that initially C54 $Ti(Si_{1-y}Ge_y)_2$ forms with a Ge index y approximately the same as the Ge index x of the $Si_{1-x}Ge_x$ substrate (i.e., $y \approx x$). After the formation of the C54 titanium germanosilicide, Si and Ge from the $Si_{1-x}Ge_x$ substrate continue to diffuse into the C54 layer, presumably via lattice and grain boundary diffusion. Some of the Si diffusing into the C54 lattice replaces Ge on the C54 lattice and the Ge index of the C54 $Ti(Si_{1-y}Ge_y)_2$ decreases (i.e., $y<x$). We propose that this process is driven by a reduction in C54 crystal energy which accompanies the replacement of Ge with Si on the C54 lattice. The excess Ge diffuses to the C54 grain boundaries where it combines with $Si_{1-x}Ge_x$ from the substrate and precipitates as $Si_{1-z}Ge_z$ which is Ge-rich relative to the substrate ($z>x$). This segregation and precipitation enhances the agglomeration of the C54 titanium germanosilicide film (i.e., lower agglomeration temperature). It was observed that rapid thermal annealing techniques could be used to reduce the annealing duration and resulted in a reduction of the Ge segregation. © *1995 American Institute of Physics.*

I. INTRODUCTION

Currently the C54 phase of titanium disilicide ($TiSi_2$) is used in microelectronics for interconnects and source and drain contacts. The C54 phase of $TiSi_2$ has a low resistivity (13–25 $\mu\Omega$ cm) and exhibits a low Schottky barrier with both p- and n-type silicon (~0.60 eV).[1] The C54 phase of $TiSi_2$ is usually formed by the solid phase reaction of Ti and Si in the multistep SALICIDE (self-aligned silicide) process.[1] The high temperature solid phase reaction of Ti with Ge can also result in the formation of a low resistivity C54 phase. The C54 phase of $TiGe_2$ forms at temperatures comparable to the C54 $TiSi_2$ formation temperature.[2,3] We have shown previously that C54 $Ti(Si_{1-y}Ge_y)_2$, isomorphic with C54 $TiSi_2$, results from the high temperature solid phase reaction of Ti and $Si_{1-x}Ge_x$ over the entire alloy composition range ($0.0 \leqslant x \leqslant 1.0$).[4] Recently, selective deposition of $Si_{1-x}Ge_x$ prior to the solid phase Ti metallization reaction has been developed as a technique for raised source and drain contacts.[5–7] This novel application and the increasing use of $Si_{1-x}Ge_x$ in device structures motivates the search for information about the metallization of this material.[8–11]

The bilayer solid phase Ti-Si and Ti-Ge reactions usually result in the formation of at least two prominent phases in each reaction. The two phases observed in the Ti-Si reaction are C49 $TiSi_2$ (base centered orthorhombic) and C54 $TiSi_2$ (face centered orthorhombic).[12–14] Several studies of the Ti-Si reaction have addressed the energetics of the C49 $TiSi_2$ formation and the C49 $TiSi_2$ to C54 $TiSi_2$ polymorphic transformation.[15,16] Recently, transmission electron microscope analysis has provided phenomenological insight into the formation and transformation processes.[17,18] The following is a summary of the Ti-Si reaction sequence:[14,17] (1) a disordered TiSi layer forms at the Ti/Si interface, (2) C49 $TiSi_2$ nucleates at the a-TiSi/Si interface and forms a continuous interface layer of C49 $TiSi_2$, (3) the C49 layer grows vertically to the surface of the sample as silicon diffuses through the C49 layer to react with the overlying Ti layer, and (4) C54 nucleates along the grain boundaries of the C49 layer and grows very rapidly. The two phases formed in the Ti-Ge solid phase reaction are Ti_6Ge_5 and C54 $TiGe_2$.[3,19,20] Initially, the Ti_6Ge_5 phase forms by diffusion controlled growth from the Ti/Ge interface, through the Ti layer, to the sample surface. At higher annealing temperatures Ge diffuses into the Ti_6Ge_5 layer and C54 $TiGe_2$ nucleates as columns extending from the Ti_6Ge_5/Ge interface to the Ti_6Ge_5 surface. The $TiGe_2$ regions then grow laterally through the Ti_6Ge_5 film. There is no analogy in the Ti-Si system for Ti_6Ge_5 and likewise C49 $TiGe_2$ has not been observed in the Ti-Ge solid phase reaction. However, Hong *et al.*[21] have observed the formation of C49 $TiGe_2$ during the recrystallization of co-deposited amorphous Ti+2Ge. The primary diffusing species in the Ti-Si and Ti-Ge reactions are Si[14] and Ge,[22] respectively. Because the intermediate phases in both systems experience diffusion controlled growth it is anticipated that the relative diffusion rates of Si and Ge in the Ti-Si_xGe_{1-x} reaction may effect the composition and structure of the intermediate phases which form. The competing energetics of the Ti-Si and Ti-Ge reaction paths may effect Ti-Si/Ti-Ge segregation during the initial stages of the reaction.

Usually when C54 $TiSi_2$ is formed from the solid phase reaction of Ti and Si, the C54 phase initially forms as a continuous layer of low resistivity C54 grains which provide

[a)]Electronic mail: Robert-Nemanich@ncsu.edu

 0021-8979/95/77(10)/5107/8/$6.00

a low resistance conduction path through the metallized layer. Following further annealing (and annealing at higher temperatures) the formation of grooves along the C54 $TiSi_2$ grain boundaries has been observed.[23] The thermal grooving of the C54 $TiSi_2$ has been modeled as a balance between the surface and grain boundary energies of the C54 $TiSi_2$ (grooving is also observed on the substrate side of the C54 grains).[14,23] Further annealing can cause the C54 grains to separate into individual islands, breaking the low resistance conduction path.[24,25] Several studies have investigated the effects of the surface and interface energetics on the shape of the agglomerated $TiSi_2$ islands. In these studies the contact angles of the $TiSi_2$ islands were used to calculated the energies of the $TiSi_2$ surface and $TiSi_2$/Si interface.[16,26]

Several studies have investigated properties of the Ti-$Si_{1-x}Ge_x$ reaction including agglomeration.[22,27–29] In a study by Ashburn *et al.*,[24,29] Ti was reacted with Si-Ge alloys by rapid thermal annealing (RTA). They found that the addition of Ge to the Ti-Si reaction lowered the temperature at which the C54 $Ti(Si_{1-y}Ge_y)_2$ grains agglomerated. An understanding of the agglomeration process of C54 $Ti(Si_{1-y}Ge_y)_2$ is necessary for determining the limits of the practical application of C54 titanium germanosilicide.

In this study Ti was reacted with $Si_{1-x}Ge_x$ ($x=0.32,0.55$) using a variety of annealing temperatures and annealing durations. The temperatures and annealing times were chosen such that the C54 $Ti(Si_{1-x}Ge_x)_2$ phase would form and then continue to react with the $Si_{1-x}Ge_x$ alloy. Structural and compositional properties were examined using x-ray diffraction (XRD), depth profile Auger electron spectroscopy (DPAES), and energy dispersive x-ray spectroscopy (EDXS). The morphologies of the surfaces and interfaces were examined using scanning electron microscopy (SEM) and cross-sectional transmission electron microscopy (XTEM). The sheet resistances of the samples were determined using four point probe measurements.

II. EXPERIMENT

To study the stability of C54 $Ti(Si_{1-y}Ge_y)_2$ formed in contact with $Si_{1-x}Ge_x$, samples were prepared using short (10 s) and long (10 min) annealing durations and a wide range of annealing temperatures. The samples annealed for long durations were prepared using an ultra-high vacuum (UHV) processing technique described below. Samples annealed for short durations were prepared using rapid thermal chemical vapor deposition (RTCVD) and RTA techniques. The range of annealing temperatures used included the C54 titanium germanosilicide formation temperature and temperatures which caused significant agglomeration of the C54 titanium germanosilicide.

The 1-in.-diam Si(100) wafers used in this study were precleaned by the manufacturer using a standard RCA cleaning procedure prior to shipment. In the laboratory the wafers were cleaned prior to use by (1) exposure to UV generated ozone to remove hydrocarbons from the surface and to form a stable oxide, (2) spin etching with a solution of hydrofluoric acid: H_2O: ethanol (1:1:10) to remove the oxide and passivate the surface with hydrogen, and (3) an *in situ* thermal desorption at >850 °C for 10 min to remove surface contaminants which may remain. This cleaning process has been shown to produce atomically clean surfaces.[30] Following the *in situ* thermal desorption at >850 °C, the substrate temperature was reduced and held at 550 °C for the deposition of a homoepitaxial silicon buffer layer (≈225 Å) and a heteroepitaxial single-crystal $Si_{0.68}Ge_{0.32}$ alloy layer (≈2500 Å). The Si buffer layer and Si-Ge layers were not intentionally doped. Silicon and germanium were codeposited from two electron beam evaporation sources. The Si and Ge deposition rates were monitored using oscillating quartz crystal monitors. Feedback from the deposition monitors was used to automatically control the relative Si and Ge deposition rates, and the maximum composition variation during deposition was approximately 2%. The compositions of the deposited $Si_{1-x}Ge_x$ alloys were determined from Rutherford backscattering (RBS) and x-ray absorption fine structure (XAFS) analysis of native $Si_{1-x}Ge_x$ layers similarly prepared.[31] Following deposition of the epitaxial $Si_{0.68}Ge_{0.32}$ alloy layer the sample was cooled to <150 °C and 400 Å of titanium was deposited from an *in situ* hot-filament Ti source. The thickness of the deposited Ti was also monitored using an oscillating quartz crystal deposition monitor. Upon completion of the titanium deposition, the samples were annealed *in situ* at temperatures of 530, 570, 660, or 700 °C. During annealing the substrate temperature was increased at a rate of 40 °C/min, held at the desired temperature for 10 min, and decreased at a rate of 40 °C/min. The processing chamber base pressure was $\sim 1\times10^{-10}$ Torr, the pressure during desorption was $<5\times10^{-10}$ Torr, the pressure during Si and Ge deposition was $<1\times10^{-8}$ Torr, the pressure during Ti deposition was $<5\times10^{-9}$ Torr, and the pressure during annealing was $<1\times10^{-9}$ Torr.

The samples prepared using RTA consisted of 3000 Å $Si_{0.45}Ge_{0.55}$ deposited by RTCVD on a chemically cleaned 4 in. Si(100) substrate.[32] A 300 Å Ti layer was subsequently sputter deposited. The 4 in. wafer was then cleaved into 1 cm^2 pieces which were RTA processed in an argon ambient at atmospheric pressure for 10 s at different temperatures. Annealing temperatures of 600, 650, 700, 850, and 900 °C were used in this study. A more detailed description of the sample preparation process has been reported previously.[28]

The structural properties of the alloys were examined using a Rigaku x-ray diffractometer. Surface and interface morphologies were examined using a JEOL 6400 field-emission scanning electron microscope and a Topcon 002B transmission electron microscope. Both the JEOL 6400 and the Topcon 002B electron microscopes were equipped with energy-dispersive x-ray spectrometers. Depth profiled Auger electron spectroscopy was used to examine compositional changes as a function of the depth in the sample. Depth profile composition measurements were performed with a JEOL JAMP-30 Auger electron microprobe system. The Auger microprobe was positioned using SEM. Auger data collection and sample sputtering were cycled until the composition of the region of interest was determined. The C, O, Ti, Si, and Ge Auger signals were monitored (in the UHV prepared samples C or O contamination was only detected on the surface of samples, apparently due to exposure of the samples to atmosphere after removal from the deposition

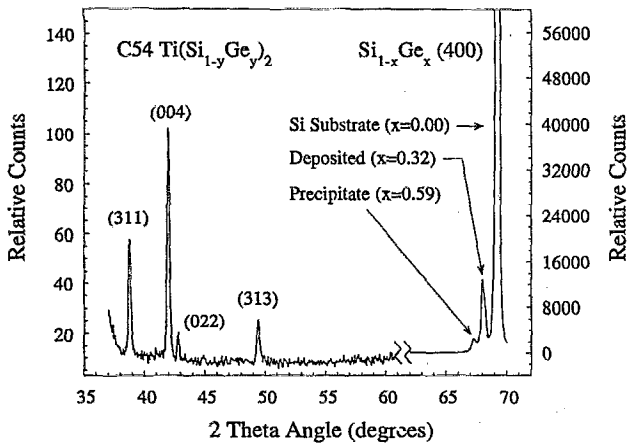

FIG. 1. XRD scan of a Ti+$Si_{0.68}Ge_{0.32}$ bilayer structure which has been annealed for 10 min at 700 °C in UHV to form C54 $Ti(Si_{1-y}Ge_y)_2$. As noted in the figure the (311), (004), (022), and (313) diffraction peaks of C54 $Ti(Si_{1-y}Ge_y)_2$ are observed. Peaks corresponding to the (400) diffraction from the Si substrate, unreacted $Si_{0.68}Ge_{0.32}$ layer, and the $Si_{0.41}Ge_{0.59}$ grain boundary decorations are also observed. The spacing of the C54 diffraction planes was calculated from the diffraction angles. The C54 lattice parameters and C54 unit cell volume were calculated from the spacing of the diffraction planes. Vegard's law was used to determine the Ge index y of the C54 $Ti(Si_{1-y}Ge_y)_2$ by comparing the calculated C54 unit cell volume to the known volumes of the C54 $TiSi_2$ and C54 $TiGe_2$ unit cells.

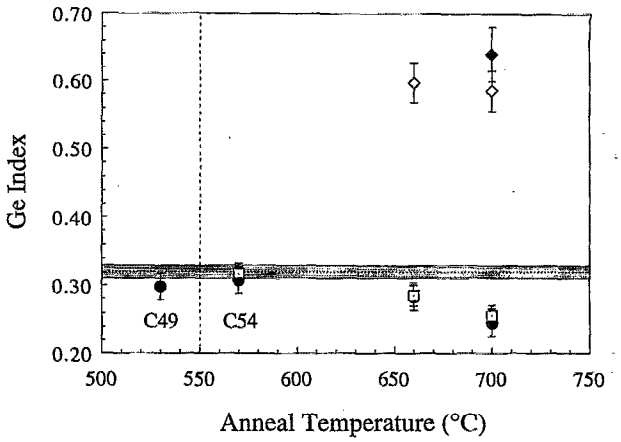

FIG. 2. Comparison of the compositions of the $Ti(Si_{1-y}Ge_y)_2$ layers and the $Si_{1-z}Ge_z$ precipitates which formed during the 10 min anneals of the Ti-$Si_{0.68}Ge_{0.32}$ bilayer samples. The Ge index x ($x=0.32\pm0.01$) of the $Si_{0.68}Ge_{0.32}$ substrate is indicated by the dashed line and gray bar. The compositions (Ge index y) of the C54 $Ti(Si_{1-y}Ge_y)_2$ layers are indicated by the circle and square symbols. The compositions (Ge index z) of the $Si_{1-z}Ge_z$ precipitates are indicated by the diamond symbols. The compositions determined by XRD analysis are indicated by the open symbols. The compositions determined by DPAES analysis are indicated by the solid symbols (DPAES analysis was only applied to the grain boundary decorations in the 700 °C sample). At 530 °C the $Ti(Si_{1-y}Ge_y)_2$ formed with a C49 structure and following annealing at higher temperatures the $Ti(Si_{1-y}Ge_y)_2$ was in the C54 structure. It appears that at the C54 $Ti(Si_{1-y}Ge_y)_2$ formation temperature the C54 $Ti(Si_{1-y}Ge_y)_2$ initially forms with the same Ge index as the $Si_{1-x}Ge_x$ substrate ($y\approx x=0.32$ in this case). As the annealing temperature increases the Ge index of the $Ti(Si_{1-y}Ge_y)_2$ decreases below the Ge index of the $Si_{0.68}Ge_{0.32}$ substrate (i.e., $y<0.32$). Also, as the annealing temperature increases, the formation of Ge-rich $Si_{1-z}Ge_z$ precipitates ($z>0.32$) is observed. The formation of Ge-rich $Si_{1-z}Ge_z$ alloy precipitates was only observed in the samples annealed at 660 and 700 °C.

system). Standard Si, Ge, Ti, and $Si_{0.68}Ge_{0.32}$ samples were used to check the relative Si, Ge, and Ti Auger sensitivities.

III. RESULTS

A. Long duration anneal—composition, morphology, and sheet resistance

XRD was used to determine the structure of the titanium germanosilicide films that formed from 10 min annealing of Ti-$Si_{0.68}Ge_{0.32}$ bilayer structures. The XRD scan of the sample annealed at 530 °C contained peaks corresponding to diffraction from the (150) and (200) planes of C49 $Ti(Si_{1-y}Ge_y)_2$. In the Ti-Si reaction C49 $TiSi_2$ is the precursor to the low resistivity C54 $TiSi_2$ phase. Apparently the addition of 32% Ge to the Si did not alter this reaction path. The XRD scans of the samples annealed at 570, 660, and 700 °C all contained peaks corresponding to diffraction from the (311), (004), (022), and (313) planes of C54 $Ti(Si_{1-y}Ge_y)_2$ (see Fig. 1). There were no indications of the presence of C49 $Ti(Si_{1-y}Ge_y)_2$ in these samples.

DPAES and XRD were used to examine the composition of the C49 and C54 titanium germanosilicides found in the samples annealed for 10 min. In a study of bulk C54 $Ti(Si_{1-y}Ge_y)_2$ by Boutarek and Madar[33] it was found that the lattice parameters of C54 titanium germanosilicide vary linearly, with respect to the Ge index y, between the lattice constants of C54 $TiSi_2$ ($y=0$) and C54 $TiGe_2$ ($y=1$) [i.e., Vegard's law holds for bulk C54 $Ti(Si_{1-y}Ge_y)_2$]. Consequently, the volume of the C54 $Ti(Si_{1-y}Ge_y)_2$ unit cell also varies linearly with respect to the Ge index y. The (311), (004), (022), and (313) diffraction peaks of the C54 found in the 570, 660, and 700 °C samples shifted to higher angle with increasing annealing temperature indicating changes in the spacing of the diffraction planes. The Ge indices of the C54 $Ti(Si_{1-y}Ge_y)_2$ in these samples were obtained by calculating the diffraction plane spacings using XRD, calculating the C54 lattice parameters from the plane spacings, calculating the volumes of the C54 unit cells, and comparing the calculated unit cell volumes with the known unit cell volumes of C54 $TiSi_2$ and C54 $TiGe_2$.[34] The C54 composition determination was based on the C54 unit cell volume (using all three lattice parameters instead of just a single lattice parameter) to reduce error which would occur if the C54 unit cell was distorted by strain. The Ge indices, as determined by DPAES and XRD, of the C49 $Ti(Si_{1-y}Ge_y)_2$ formed at 530 °C and the C54 $Ti(Si_{1-y}Ge_y)_2$ formed at 570, 660, and 700 °C are plotted in Fig. 2. The Ge indices determined by DPAES and XRD are in good agreement. The Ge indices of the samples annealed at 530 and 570 °C, as determined by DPAES analysis, are approximately equal to the Ge index of the deposited $Si_{0.68}Ge_{0.32}$ alloy (i.e., $y\approx0.32$). At the higher annealing temperatures of 660 and 700 °C, the observed decrease in the Ge index indicates that Ge in the C54 $Ti(Si_{1-y}Ge_y)_2$ is being replaced by Si (i.e., $y<0.32$).

Scanning electron micrographs of the surface morphologies of the samples annealed at 660 and 700 °C are shown in Fig. 3. After annealing at 660 °C the formation of decorations along the C54 grain boundaries was observed [Fig. 3(a)]. An increase in the average size and areal density of the decorations was observed for the sample annealed at 700 °C

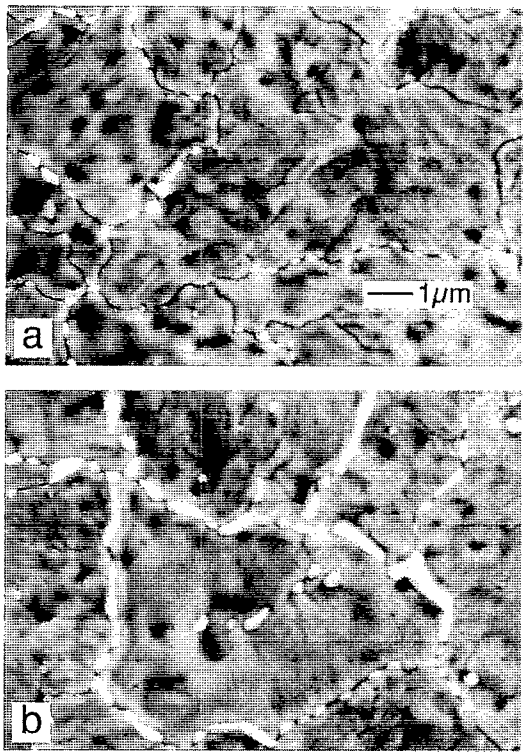

FIG. 3. SEM micrographs of the morphology of the samples annealed for 10 min at 660 and 700 °C. After annealing at 660 °C $Si_{1-z}Ge_z$ decorations are observed along the C54 $Ti(Si_{1-y}Ge_y)_2$ grain boundaries (a). After annealing at 700 °C the grain boundary decorations occupy a significant portion of the C54 grain boundaries (b). The largest decorations appear to have formed at C54 triple grain boundaries.

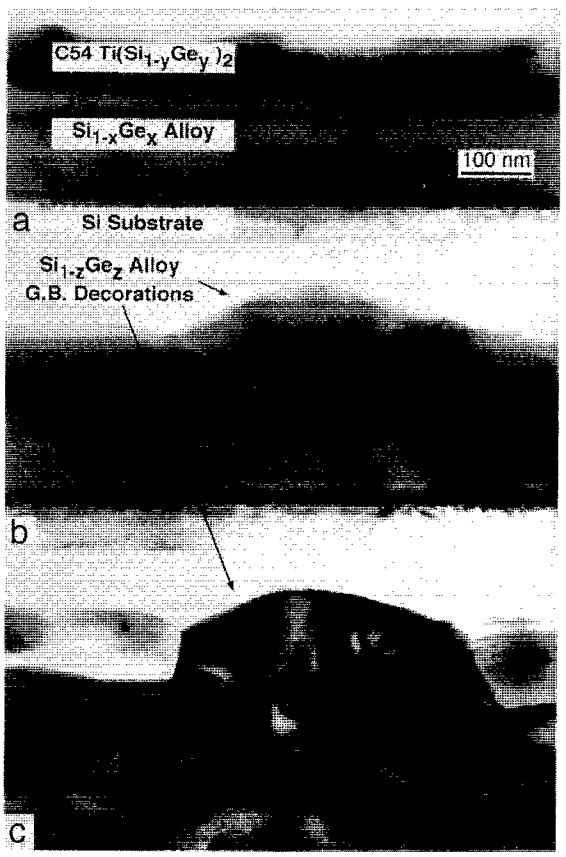

FIG. 4. Cross-section TEM micrographs of a C54 $Ti(Si_{1-y}Ge_y)_2$ grain and $Si_{1-z}Ge_z$ grain boundary decorations found in the 700 °C UHV sample. (a) Cross section of the C54 $Ti(Si_{1-y}Ge_y)_2$ grain showing the relatively smooth surface and an abrupt $C54/Si_{0.68}Ge_{0.32}$ interface. (b) A conical sidewall $Si_{1-z}Ge_z$ precipitate on a C54 grain boundary. (c) A vertical sidewall $Si_{1-z}Ge_z$ precipitate on a C54 grain boundary.

[Fig. 3(b)]. A close inspection of the two samples revealed that the largest decorations formed at triple (or greater) grain boundary intersections. The high energy of such grain boundary intersections may promote the nucleation of decorations at these sites. Energy dispersive x-ray spectroscopy in the SEM was used to examine the composition of the C54 grains and the grain boundary decorations. Within the EDXS detection limit no Ti was found in the decorations. Grain boundary decorations were not observed in the samples annealed at 530 or 570 °C.

The morphology of the C54 grains and the grain boundary decorations of the 700 °C sample were more closely examined using XTEM. As is shown in Fig. 4(a) the C54 titanium germanosilicide formed with a relatively smooth surface and an abrupt $C54/Si_{0.68}Ge_{0.32}$ interface. Two different geometries of the grain boundary decorations were observed (angled sidewalls and vertical sidewalls). As shown in Figs. 4(b) and 4(c) both types of decorations extend from the sample surface to the underlying $Si_{0.68}Ge_{0.32}$ alloy layer, effectively separating the two neighboring C54 grains.

The top surfaces of the grain boundary decorations are convex and the apex of the convex surfaces are higher than the original surface of the C54 $Ti(Si_{1-y}Ge_y)_2$ grains. A nanoprobe was focused on the decorations, the underlying $Si_{1-x}Ge_x$ alloy layer, and the silicon substrate for microdiffraction and EDXS analysis in the TEM. The microdiffraction analysis of the microstructure detected the diamond structure in all three of the areas. A slight difference in the lattice spacings in the three areas was also detected. The largest lattice spacing was measured in the decorations and the smallest lattice spacing was measured in the Si substrate indicating that the decorations ($Si_{1-z}Ge_z$) were richer in Ge than the underlying $Si_{1-x}Ge_x$ alloy ($z>x$). Dislocations starting at the decoration/alloy-layer and alloy-layer/Si substrate interfaces were observed [see Fig. 4(c)], indicative of the lattice mismatch between these regions due to the different Ge concentrations. The EDXS results also indicated that the decoration area was richer in Ge than the underlying $Si_{1-x}Ge_x$ alloy layer.

The composition of the grain boundary decorations was also examined using DPAES and XRD. The XRD scans of these samples included the range where the Si (400), Ge (400), and $Si_{1-x}Ge_x$ (400) diffraction peaks occur, as shown in Fig. 1. At 530 and 570 °C, the only XRD peaks observed in this range corresponded to the Si substrate and the remaining unreacted $Si_{0.68}Ge_{0.32}$ alloy. At 660 and 700 °C, an additional peak corresponding to $Si_{0.41}Ge_{0.59}(z=0.59\pm0.04)$ was observed. DPAES was also used to examine the composition of the decorations along C54 grain boundaries. The DPAES analysis indicated that the Ge index z of the $Si_{1-z}Ge_z$ grain boundary decorations in the 700 °C annealed sample was $z=0.64\pm0.04$, in good agreement with the

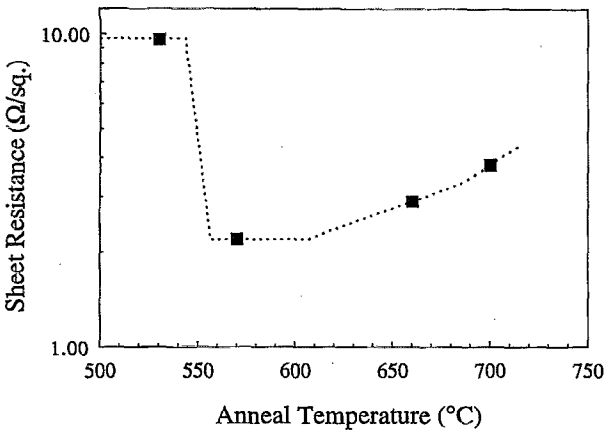

FIG. 5. Measured sheet resistance of the samples annealed for 10 min. At 530 °C the $Ti(Si_{1-y}Ge_y)_2$ is in the high resistivity C49 phase. At 570 °C the $Ti(Si_{1-y}Ge_y)_2$ has transformed to the low resistivity C54 phase. At 660 and 700 °C grain boundary decorations form along the C54 grain boundaries and the sheet resistance increases. The dashed line is included to guide the eye and is not an extrapolation of the data.

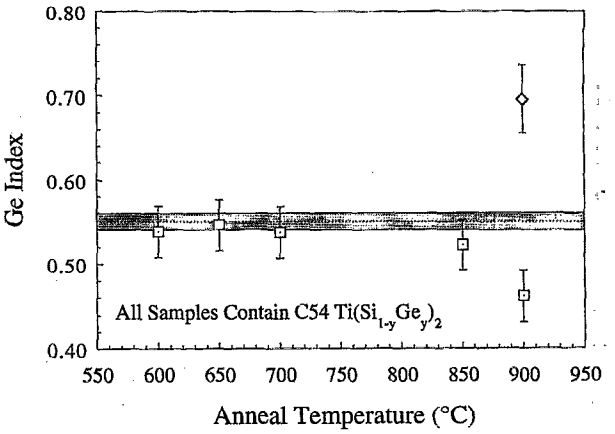

FIG. 6. Comparison of the compositions of the C54 $Ti(Si_{1-y}Ge_y)_2$ layers and the $Si_{1-z}Ge_z$ precipitates which formed during the 10 s annealing of the Ti-$Si_{0.45}Ge_{0.55}$ bilayer samples. The Ge index x ($x=0.55\pm0.01$) of the $Si_{0.45}Ge_{0.55}$ substrate is indicated by the dashed line and gray bar. The compositions (Ge index y) of the C54 $Ti(Si_{1-y}Ge_y)_2$ layers are indicated by the open squares. The composition (Ge index z) of the $Si_{1-z}Ge_z$ alloy, which was detected at high annealing temperature, is indicated by the open diamond. The compositions were determined by XRD analysis. It appears that at the C54 formation temperature the C54 $Ti(Si_{1-y}Ge_y)_2$ forms with the same Ge index as the $Si_{0.45}Ge_{0.55}$ substrate (i.e., $y\approx0.55$). The formation of C54 $Ti(Si_{1-y}Ge_y)_2$ was first detected after annealing at 600 °C. An appreciable change in the Ge index of the C54 $Ti(Si_{1-y}Ge_y)_2$ was not detected until the annealing temperature was increased to >850 °C. It appears that the segregation of Ge out of the C54 $Ti(Si_{1-y}Ge_y)_2$ is limited by the short annealing duration.

XRD results. The Ge index of the grain boundary decorations are also plotted in Fig. 2.

The sheet resistances of the long duration anneal samples were measured and are displayed in Fig. 5. The sheet resistance after annealing at 530 °C is 9.6 Ω/□. This corresponds to the high resistivity C49 phase of the $Ti(Si_{1-y}Ge_y)_2$. At 570 °C, the $Ti(Si_{1-y}Ge_y)_2$ transformed to the low resistivity C54 phase and the sheet resistance dropped to 2.2 Ω/□. At 660 and 700 °C, the temperatures where Ge segregation and grain boundary decorations were observed, the sheet resistance increases to 2.9 and 3.8 Ω/□, respectively.

B. Short duration anneal—composition

The compositions of the C54 $Ti(Si_{1-y}Ge_y)_2$ layers resulting from the RTA (10 s anneal) reactions of Ti with a $Si_{0.45}Ge_{0.55}$ substrate were determined using similar XRD analysis. The Ge indices of the C54 titanium germanosilicides found in the short duration anneal samples are plotted in Fig. 6. The Ge indices of the C54 $Ti(Si_{1-y}Ge_y)_2$ layers in these samples closely match the Ge index of the deposited $Si_{0.45}Ge_{0.55}$ alloy for temperatures below 850 °C (i.e., $y\approx0.55$). At 850 °C, the Ge index of the C54 layer is slightly reduced and at 900 °C the Ge index is significantly reduced ($y\approx0.46$). The XRD scans of these samples also included the range where the Si (400), Ge (400), and $Si_{1-x}Ge_x$ (400) diffraction peaks occur. The only diffraction peaks observed in the XRD scans of samples annealed below 900 °C were due to the C54 $Ti(Si_{1-y}Ge_y)_2$, the deposited $Si_{0.45}Ge_{0.55}$ alloy, and the Si substrate. At 900 °C, an additional peak corresponding to the (400) diffraction from $Si_{0.30}Ge_{0.70}$ was also observed (Fig. 6). These results are similar to those of the samples annealed for 10 min. However, in the samples annealed for 10 s the C54 titanium germanosilicide appears to be stable at higher temperatures with respect to Ge migration out of the C54 structure.

IV. DISCUSSION

The measured C54 compositions, for both the short and long duration annealed samples, indicate that the $Ti+Si_{1-x}Ge_x \Rightarrow C54\ Ti(Si_{1-y}Ge_y)_2+Si_{1-z}Ge_z$ ($y<x<z$) reaction can be separated into a two step process: (1) C54 formation and (2) germanium segregation [Eqs. (1) and (2), respectively]

$$Ti+Si_{1-x}Ge_x \Rightarrow C54\ Ti(Si_{1-x}Ge_x)_2, \tag{1}$$

$$C54\ Ti(Si_{1-x}Ge_x)_2+Si_{1-x}Ge_x \Rightarrow C54\ Ti(Si_{1-y}Ge_y)_2+Si_{1-z}Ge_z \quad (y<x<z). \tag{2}$$

In the plots of C54 composition versus annealing temperature, for both the short and long duration annealed samples (Figs. 2 and 6, respectively) it appears that at the C54 formation temperature the C54 $Ti(Si_{1-y}Ge_y)_2$ forms with the same Ge index as the deposited $Si_{1-x}Ge_x$ layer (i.e., $y=x$). As the annealing temperature is increased, Ge on the C54 lattice is replaced by Si and the Ge index of the C54 $Ti(Si_{1-y}Ge_y)_2$ decreases ($y<x$). The decrease in the Ge index of the C54 titanium germanosilicide occurs concurrently with the observed formation of Ge-rich $Si_{1-z}Ge_z$ alloy grain boundary decorations ($z>x$).

In both the Ti-Si and Ti-Ge reactions the formation of the final C54 phase is nucleation controlled and is driven by a reduction in crystal energy which occurs when the C54 phase forms.[18,19] Presumably the same is true of the Ti-$Si_{1-x}Ge_x$ reaction. In this study, it was found that when the C54 $Ti(Si_{1-y}Ge_y)_2$ initially formed, the C54 had approximately the same Ge index as the $Si_{1-x}Ge_x$ alloy of the sub-

strate ($y=x$). This indicates that at near the C54 formation temperature the driving force for the C54 phase formation is much greater than the driving force for the Ge segregation. The initial formation of C54 $Ti(Si_{1-x}Ge_x)_2$ from the $Ti+Si_{1-x}Ge_x$ reaction is consistent with the results of a study of bulk Ti-Si-Ge by Boutarek and Madar.[33] In that study it was found that C54 $TiSi_2$ and C54 $TiGe_2$ are completely miscible when the quantities of Ti, Si, and Ge are limited to Ti:(Si+Ge)=1:2.

Following the formation of the C54 $Ti(Si_{1-x}Ge_x)_2$ on $Si_{1-x}Ge_x$, Si and Ge are available from the underlying $Si_{1-x}Ge_x$ substrate for continued reaction with the C54 layer. If it is assumed that Si and Ge diffuse into the C54 layer in quantities proportional to the $Si_{1-x}Ge_x$ alloy composition then the replacement of Ge with Si on the C54 lattice, as observed in the compositional analysis, will result in a large excess of Ge in the C54 lattice. The binary phase diagram of Ti and Si indicates a very limited solubility of Si in C54 $TiSi_2$.[35] Presumably the solid solubilities of Si and Ge in C54 $Ti(Si_{1-y}Ge_y)_2$ will also be very limited. The limited solubilities indicate that the C54 titanium germanosilicide cannot support a large excess of dissolved Ge. The buildup of dissolved Ge in the C54 titanium germanosilicide will limit the progression of the replacement of Ge with Si on the C54 lattice. Some of the excess Ge could diffuse out of the C54 lattice and into C54 grain boundaries, but a high concentration of mobile Ge in the grain boundaries would limit the net diffusion of Ge out of the C54 lattice which would again limit the Ge/Si replacement reaction occurring in the C54. The compositional analysis (Figs. 2 and 6) indicates that excess Ge which diffuses to the C54 grain boundaries can combine with Si and Ge from the substrate and nucleate as Ge-rich $Si_{1-z}Ge_z$ ($z>x$). The nucleation of $Si_{1-z}Ge_z$ at the C54 grain boundaries establishes a sink for excess Ge and enables the replacement of Ge with Si on the C54 lattice to continue. A schematic representation of this reaction sequence appears in Fig. 7.

The diffusion of Ge in C54 $TiSi_2$ has been studied by Gas *et al.*[36] In that study Ge was implanted into a C54 $TiSi_2$ layer which was subsequently annealed to examine the diffusion of the Ge. The lattice diffusion coefficients were determined and it was found that Ge diffused along the C54 $TiSi_2$ grain boundaries more rapidly than through the C54 $TiSi_2$ lattice. The results of Gas *et al.* suggest that in this study: (1) Si and Ge from the $Si_{1-x}Ge_x$ substrate diffuse more rapidly into and along the C54 titanium germanosilicide grain boundaries; and (2) the subsequent diffusion of Si into the C54 lattice, the replacement of Ge with Si on the C54 lattice, and the diffusion of Ge out of the C54 lattice occurs at a slower rate. This is consistent with the formation of $Si_{1-z}Ge_z$ along the grain boundaries where the excess Ge diffusing out of the C54 lattice combines with Si and Ge diffusing into the grain boundary from the $Si_{1-x}Ge_x$ alloy substrate ($z>x$).

A possible driving force for the segregation of Ge from the C54 lattice can be found in the relative crystal energies of the C54 $TiSi_2$ and C54 $TiGe_2$ structures. If the heats of formation of C54 $TiSi_2$ and C54 $TiGe_2$ are used as an approximation of the relative crystal energies of these materials, then

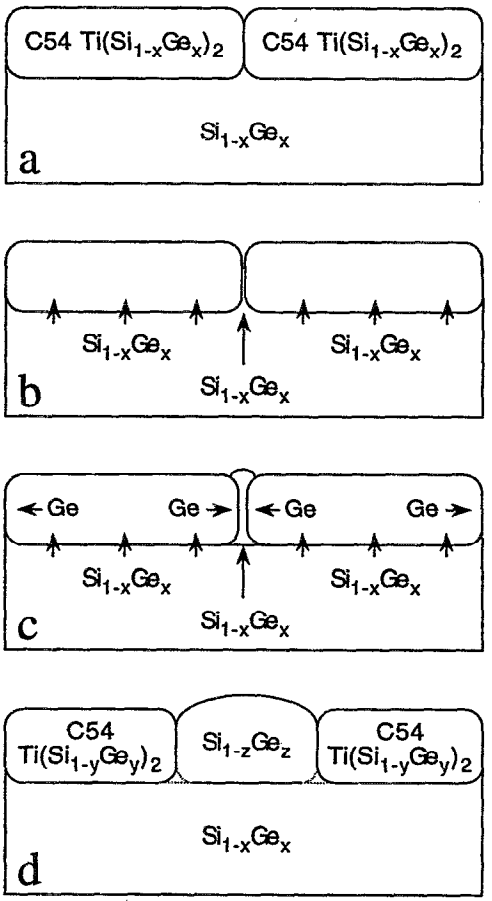

FIG. 7. Schematic representation of the reaction of C54 $Ti(Si_{1-x}Ge_x)_2$ with $Si_{1-x}Ge_x$. Initially the C54 $Ti(Si_{1-x}Ge_x)_2$ is formed from the solid phase reaction of Ti and $Si_{1-x}Ge_x$ (a). After the C54 phase forms, silicon and germanium from the substrate diffuses into the C54 lattice and into the C54 grain boundaries (b). Driven by a reduction of the crystal energy, the diffusing Si replaces Ge on the C54 lattice. The excess Ge diffuses to the C54 grain boundary where it combines with Si and Ge from the substrate and precipitates as $Si_{1-z}Ge_z$ ($z>x$), (c). As the diffusion continues the Ge index of the C54 $Ti(Si_{1-y}Ge_y)_2$ decreases ($y<x$) and the size of the $Si_{1-z}Ge_z$ nuclei increases, (d).

the relative stability of these two materials can be compared. The heats of formation of C54 $TiSi_2$ and C54 $TiGe_2$ have been determined to be -57.0 and -47.5 kJ/mol, respectively.[37–39] These values suggest that given C54 $TiGe_2$, the crystal energy could be reduced if the Ge atoms could be replaced by Si atoms. An approximation for the heat of formation (i.e., crystal energy) of C54 $Ti(Si_{1-x}Ge_x)_2$ is a linear interpolation between the C54 $TiSi_2$ and C54 $TiGe_2$ end point values, or

$$\Delta H(x)=(9.5\ \text{kJ/mol})x-(57.0\ \text{kJ/mol}). \tag{3}$$

Equation (3) suggests that for the C54 titanium germanosilicide crystal, the replacement of Ge with Si will reduce the C54 crystal energy. This linear approximation is also consistent with the complete miscibility of C54 $TiSi_2$ and C54 $TiGe_2$ observed by Boutarek and Madar.[33] Using the linear approximation [Eq. (3)] the crystal energies on both sides of Eq. (4) are balanced

$$A\ \mathrm{Ti(Si_{1-x}Ge_x)_2} = A(1-x)\mathrm{TiSi_2} + Ax\ \mathrm{TiGe_2} \quad (4)$$

(where all three compounds have the C54 crystal structure and A is the total quantity of C54) and there is no crystal energy driving force for segregation of C54 $TiSi_2$ and C54 $TiGe_2$.

In the experimental results there is a direct correlation between the appearance of $Si_{1-z}Ge_z$ decorations [Ge-rich relative to the $Si_{1-x}Ge_x$ substrate ($z>x$)] along the C54 titanium germanosilicide grain boundaries and an increase in the sheet resistance of the sample. This correlation suggests that the segregation of Ge out of the C54 titanium germanosilicide may promote the agglomeration of the C54 grains and lead to an interruption of the low resistance conduction path through the C54 layer. In the samples annealed for 10 s higher annealing temperatures were required to produce a measurable change in the C54 $Ti(Si_{1-y}Ge_y)_2$ composition and the formation of detectable $Si_{1-z}Ge_z$ nuclei. This effect of annealing duration suggests that by limiting the annealing duration the diffusion of Si into and Ge out of the C54 grains can be limited. The presence of contamination at the $Ti/Si_{0.45}Ge_{0.55}$ interface and in the Ti prior to annealing may also contribute to the stability of the short duration annealed (rapid thermal processed) samples.

The segregation of Ge out of C54 $Ti(Si_{1-y}Ge_y)_2$ requires the transport of material and appears to be a thermally activated process [i.e., no segregation is observed at low temperatures when C54 $Ti(Si_{1-y}Ge_y)_2$ first forms and the rate of segregation increases with annealing temperature]. In both sets of samples (10 s anneal with $x=0.55$ and 10 min. anneal with $x=0.32$) it was observed that the C54 $Ti(Si_{1-y}Ge_y)_2$ formed from the Ti-$Si_{1-x}Ge_x$ reaction initially formed with $y \approx x$. The composition of the initial C54 $Ti(Si_{1-y}Ge_y)_2$ seems to be directly correlated to the composition of the underlying $Si_{1-x}Ge_x$ alloy and independent of the annealing duration and annealing temperature ramp rate. We suggest that after the formation of the initial C54 $Ti(Si_{1-y}Ge_y)_2$ ($y \approx x$) then Eq. (3) defines the thermodynamic driving force for Ge segregation, and the rate or degree of Ge segregation is controlled by the nucleation of the $Si_{1-z}Ge_z$ grain boundary decorations and the mobility of the Si and Ge atoms. It is anticipated that the alloy composition may also effect the rate or degree of Ge segregation from C54 $Ti(Si_{1-y}Ge_y)_2$. But presumably, the effect of composition will not completely account for the $\approx$240 °C difference between the $Si_{1-z}Ge_z$ precipitation temperatures observed for the samples annealed for 10 min. ($x=0.32$, Fig. 2) and the samples annealed for 10 s ($x=0.55$, Fig. 6).

V. CONCLUSIONS

The formation and stability of C54 $Ti(Si_{1-y}Ge_y)_2$ formed from the solid phase reaction of Ti with $Si_{1-x}Ge_x$ has been investigated (specifically $x=0.32$ and 0.55). The reaction can be separated into two stages: $Ti+Si_{1-x}Ge_x \Rightarrow$ C54 $Ti(Si_{1-x}Ge_x)_2$ and C54 $Ti(Si_{1-x}Ge_x)_2+Si_{1-x}Ge_x \Rightarrow$ C54 $Ti(Si_{1-y}Ge_y)_2+Si_{1-z}Ge_z$ where $y<x<z$. The driving force for the C54 titanium germanosilicide formation is a decrease in the crystal energy which accompanies the C54 phase formation. After the initial C54 $Ti(Si_{1-x}Ge_x)_2$ formation, Si and Ge from the $Si_{1-x}Ge_x$ substrate continue to diffuse into the C54 layer via lattice and grain boundary diffusion. A reduction in crystal energy drives the replacement of Ge with Si in the C54 lattice and the Ge index y of the C54 $Ti(Si_{1-y}Ge_y)_2$ decreases ($y<x$). The excess Ge diffusing out of the C54 lattice combines with the Si and Ge diffusing into the C54 grain boundaries from the substrate and nucleates as $Si_{1-z}Ge_z$ ($z>x$) along the grain boundaries.

The degree of Ge segregation appears to be related to the mobility of Si and Ge in the C54 region. For a given temperature the degree of Ge segregation was reduced by reducing the annealing duration using rapid thermal annealing. Decreasing the annealing duration required increasing the annealing temperature to produce significant Ge segregation and the formation of detectable $Si_{1-z}Ge_z$ nuclei. Limiting the duration of the reaction appears to limit the transport of Si into and Ge out of the C54 layer, increasing the stability of the C54 $Ti(Si_{1-y}Ge_y)_2$.

ACKNOWLEDGMENTS

The authors would like to thank Dr. George Rozgonyi and Dr. Dennis Maher for their assistance with XRD and TEM analysis, respectively, and thoughtful scientific discussion. This work was supported in part by the National Science Foundation through Grant No. DMR 9204285 and by the Division of Materials Science of the Department of Energy under Contract No. DE-FG05-89ER45384.

[1] S. P. Murarka, *Metallization: Theory and Practice for VLSI and ULSI* (Butterworth–Heinemann, Boston, 1993).
[2] O. Thomas, S. Delage, F. M. d'Heurle, and G. Scilla, Appl. Phys. Lett. **54**, 228 (1989).
[3] D. B. Aldrich, C. L. Jahncke, R. J. Nemanich, and D. E. Sayers, in *Heteroepitaxy of Dissimilar Materials*, edited by R. F. C. Farrow, J. P. Harbison, P. S. Peercy, and A. Zangwill (Materials Research Society, Pittsburgh, 1991), Vol. 221, pp. 343–348.
[4] D. B. Aldrich, R. J. Nemanich, and D. E. Sayers, in *Proceedings of the Seventh International Conference on X-ray Absorption Fine Structure*, edited by H. Kuroda, T. Ohta, T. Murata, Y. Udagawa, and M. Nomura [Jpn. J. Appl. Phys. Tokyo (1993)], Vol. 32, Suppl. 32-2, pp. 725–727.
[5] S. P. Ashburn, D. T. Grider, and M. C. Öztürk, J. Appl. Phys. **74**, 4455 (1993).
[6] D. T. Grider, M. C. Öztürk, J. J. Wortman, G. S. Harris, and D. M. Maher, in *Rapid Thermal and Integrated Processing II*, edited by J. C. Gelpey, J. K. Elliott, J. J. Wortman, and A. Ajmera (Materials Research Society, Pittsburgh, 1993), Vol. 303, pp. 31–36.
[7] X. Ren, M. C. Öztürk, D. T. Grider, M. Sanganeria, and S. Ashburn, in Ref. 6, pp. 37–41.
[8] J. C. Sturm, E. J. Prinz, and C. W. Magee, IEEE Electron Device Lett. **EDL-12**, 303 (1991).
[9] P. M. Garone, V. Venkataraman, and J. C. Sturm, IEDM Tech. Digest **90**, 383 (1990).
[10] T.-J. King, K. C. Saraswat, and J. R. Pfiester, IEEE Electron Device Lett. **EDL-12**, 584 (1991).
[11] T. J. King, J. R. Pfiester, J. D. Shott, J. P. McVitte, and K. C. Saraswat, IEDM Tech. Digest **90**, 253 (1990).
[12] *Pearson's Handbook of Crystallographic Data for Intermetallic Phases*, edited by P. Villars and L. D. Calvert (ASM International, Metals Park, OH, 1991).
[13] S. P. Murarka, *Silicides for VLSI Applications* (Academic, New York, 1983).
[14] K. Maex, Mater. Sci. Eng. R **11**, 53 (1993).
[15] H. Jeon and R. J. Nemanich, Thin Solid Films **184**, 357 (1990).
[16] H. Jeon, C. A. Sukow, J. W. Honeycutt, G. A. Rozgonyi, and R. J. Nemanich, J. Appl. Phys. **71**, 4269 (1992).

[17] Z. Ma, Y. Xu, L. H. Allen, and S. Lee, J. Appl. Phys. **74**, 2954 (1993).
[18] Z. Ma and L. H. Allen, Phys. Rev. B **49**, 13501 (1994).
[19] O. Thomas, F. M. d'Heurle, S. Delage, and G. Scilla, Appl. Surf. Sci. **38**, 27 (1989).
[20] S. P. Ashburn, M. C. Öztürk, J. J. Wortman, G. Harris, J. Honeycutt, and D. M. Maher, J. Electron. Mater. **21**, 81 (1992).
[21] Q. Z. Hong, K. Barmak, and F. M. d'Heurle, Appl. Phys. Lett. **62**, 3435 (1993).
[22] O. Thomas, F. M. d'Heurle, and S. Delage, J. Mater. Res. **5**, 1453 (1990).
[23] T. P. Nolan, R. Sinclair, and R. Beyers, J. Appl. Phys. **71**, 720 (1992).
[24] S. P. Ashburn, M. C. Öztürk, G. Harris, and D. M. Maher (unpublished).
[25] S.-i. Ogawa, T. Yoshida, and T. Kouzaki, Appl. Phys. Lett. **56**, 725 (1990).
[26] C. A. Sukow and R. J. Nemanich, J. Mater. Res. **9**, 1214 (1994).
[27] D. B. Aldrich, Y. L. Chen, D. E. Sayers, and R. J. Nemanich, in *Silicides, Germanides, and Their Interfaces*, edited by R. W. Fathauer, S. Mantl, L. J. Schowalter, and K. N. Tu (Materials Research Society, Pittsburgh, 1994), Vol. 320, pp. 305–310.
[28] S. P. Ashburn, M. C. Öztürk, G. Harris, D. M. Maher, D. B. Aldrich, and R. J. Nemanich (unpublished).
[29] S. P. Ashburn, Dissertation thesis, North Carolina State University (1994).
[30] H. Jeon, C. A. Sukow, J. W. Honeycutt, T. P. Humphreys, R. J. Nemanich, and G. A. Rozgonyi, in *Advanced Metallizations in Microelectronics*, edited by A. Katz, S. P. Murarka, and A. Appelbaum (Materials Research Society, Pittsburgh, 1990), Vol. 181, pp. 559–564.
[31] D. B. Aldrich, R. J. Nemanich, and D. E. Sayers, Phys. Rev. B **50**, 15026 (1994).
[32] Y. Zhong, M. C. Öztürk, D. T. Grider, J. J. Wortman, and M. A. Littlejohn, Appl. Phys. Lett. **57**, 2092 (1990).
[33] N. Boutarek and R. Madar, Appl. Surf. Sci. **73**, 209 (1993).
[34] D. B. Aldrich, D. E. Sayers, and R. J. Nemanich, in *Evolution of Surface and Thin Film Microstructure*, edited by H. A. Atwater, E. Chason, M. H. Grabow, and M. G. Lagally (Materials Research Society, Pittsburgh, 1993), Vol. 280, pp. 585–588.
[35] *Binary Alloy Phase Diagrams*, edited by T. B. Massalski (ASM International, Materials Park, OH, 1990), Vol. 3.
[36] P. Gas, G. Scilla, A. Michel, F. K. LeGoues, O. Thomas, and F. M. d'Heurle, J. Appl. Phys. **63**, 5335 (1988).
[37] M. E. Schlesinger, Chem. Rev. **90**, 607 (1990).
[38] *Cohesion in Metals: Transition Metal Alloys*, edited by F. R. deBoer, R. Boom, W. C. M. Mattens, A. R. Miedema, and A. K. Niessen (North-Holland, New York, 1988).
[39] R. Pretorius, T. K. Marais, and C. C. Theron, Mater. Sci. Eng. **10**, 1 (1993).